Electronic Supplemental Information

Amino alcohols and benzoates-Friends or foes? Tuning nuclearity of Cu(II) complexes, structures, magnetism, DFT and TD-DFT studies, and catecholase like activities

Farasha Sama, Ashish Kumar Dhara, Muhammad Nadeem Akhtar, Yan-Cong Chen, Ming-Liang Tong, Iftikhar A. Ansari, Mukul Raizada, Musheer Ahmad, M. Shahid, Zafar A. Siddiqi
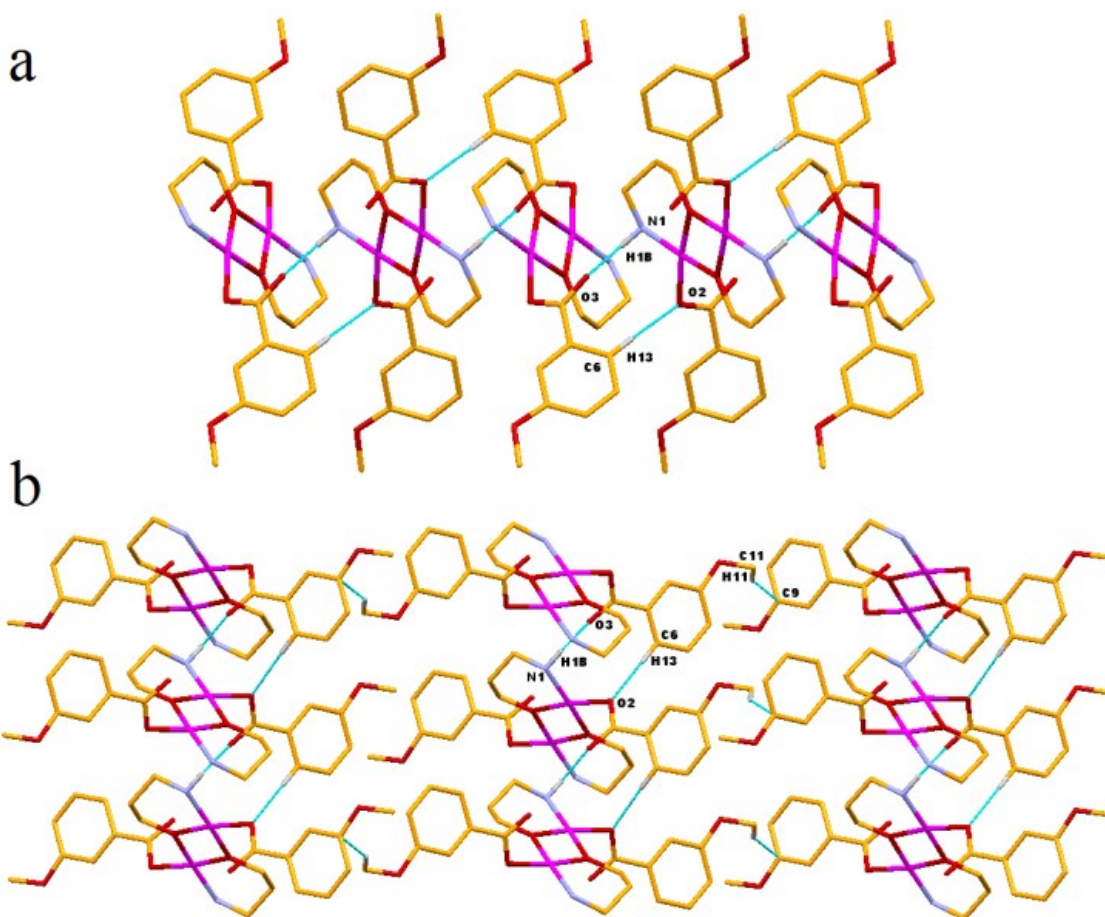

Fig. S1. (a) Formation of 1D chain by N–H···O and C–H···O interactions in **2**. (b) Formation of 2D network by various O···H and C–H···π interactions in **2**.
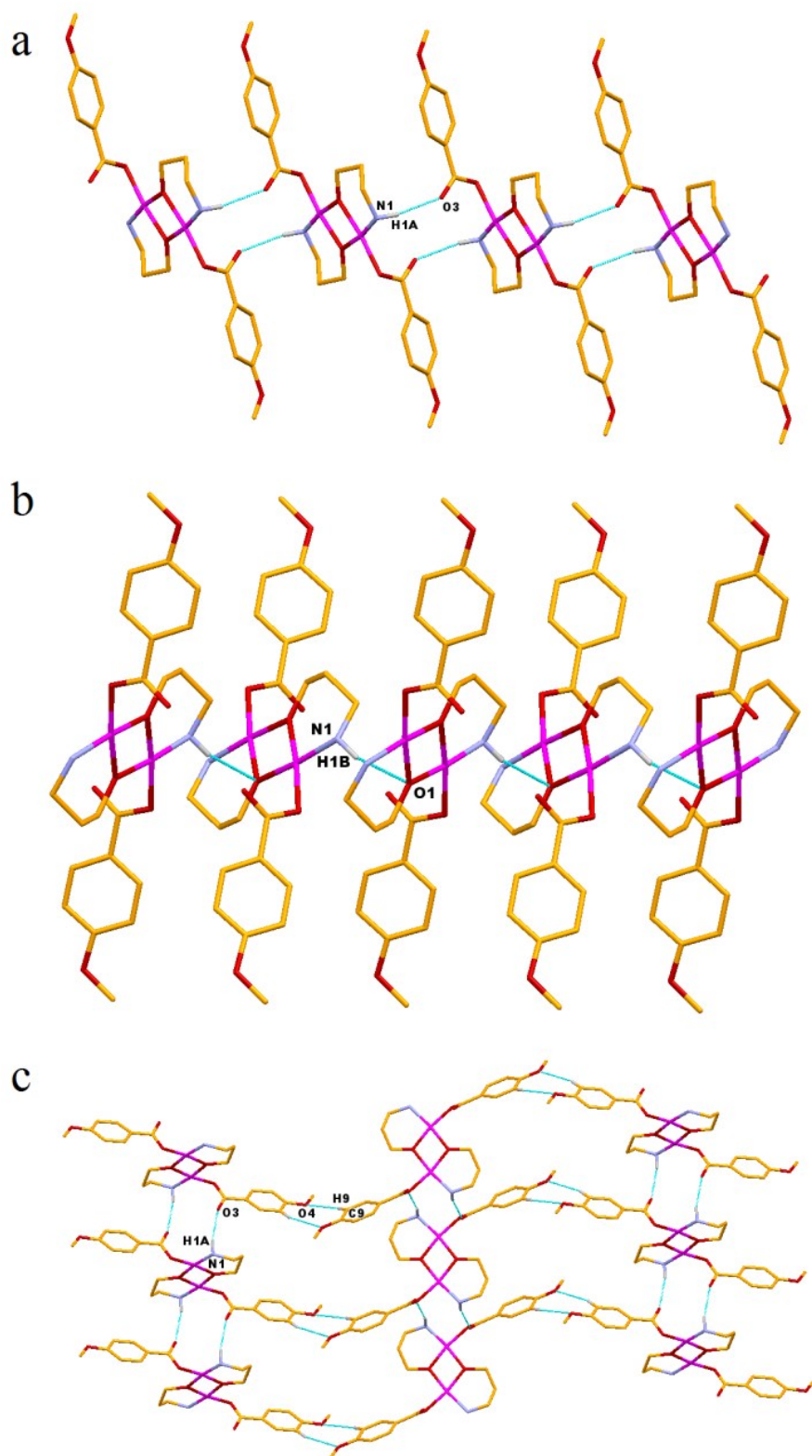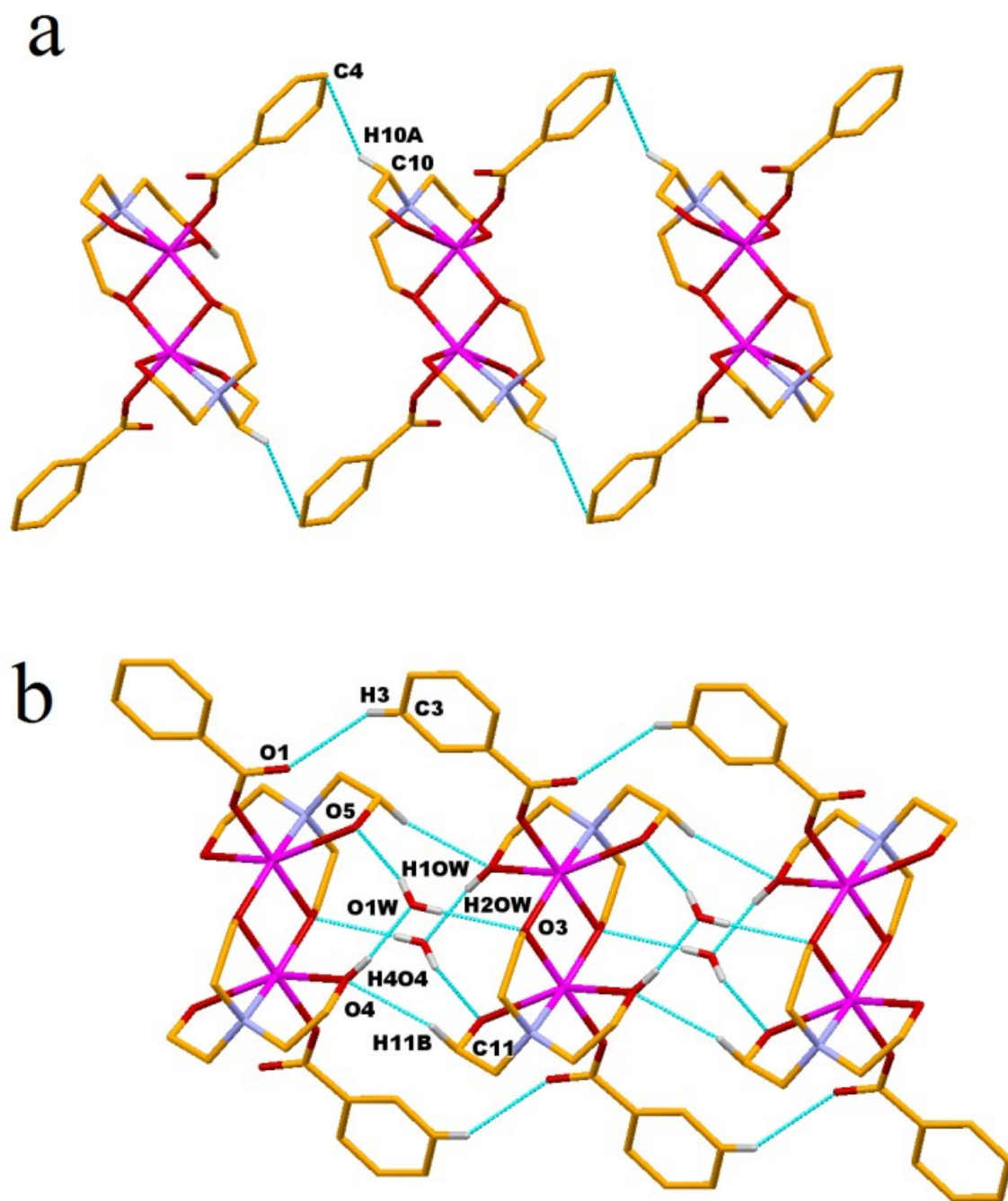
Fig. S2. (a) Formation of 1D chain as a result of N–H···O interactions in **3**. (b) Formation of zigzag 2D sheet network by various O···H interactions in **3**.
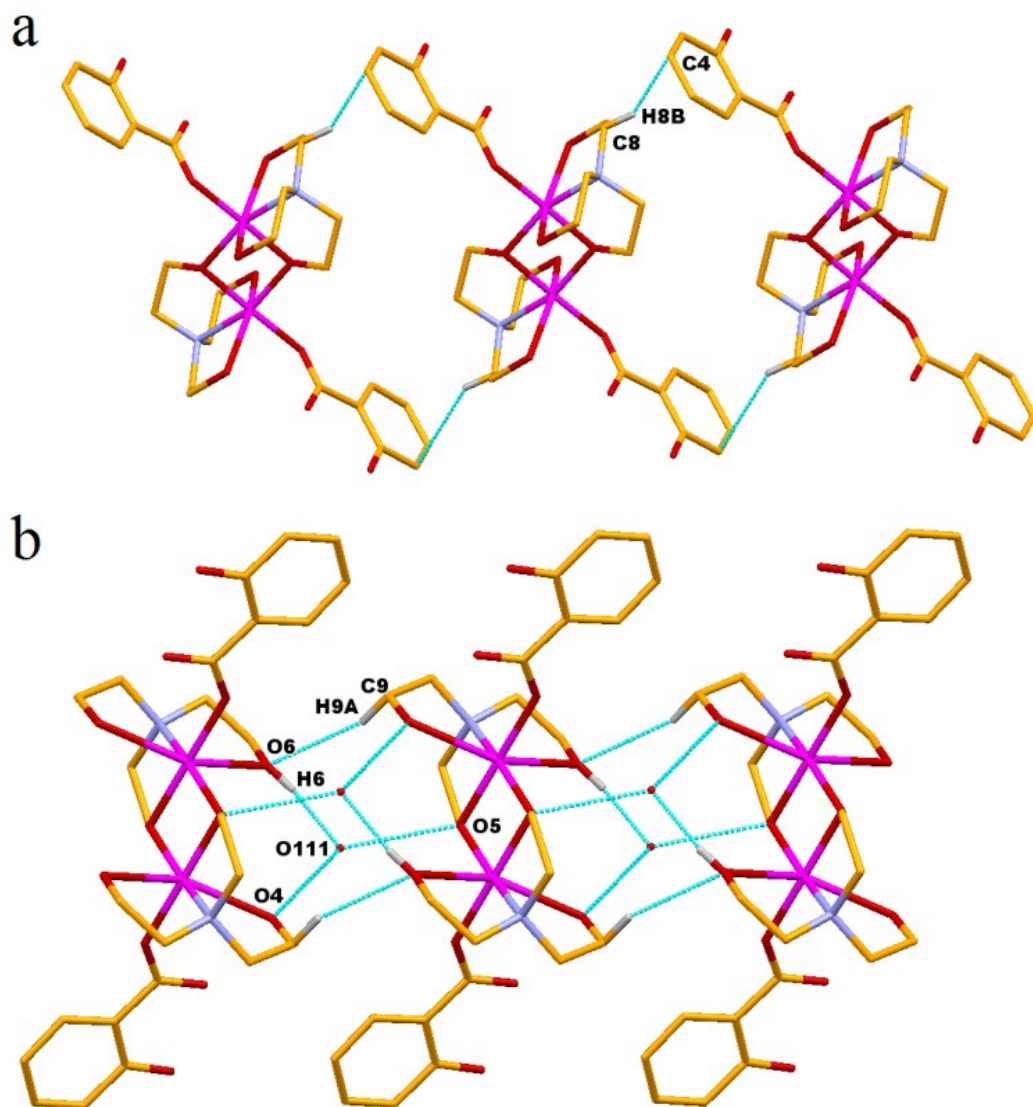
Fig.S3. (a) Formation of 1D chain by C–H···π interactions in **4**. (b) Formation of 1D chain by water of crystallization in **4**.

Fig. S4. (a) Formation of 1D chain by C–H···π interactions in **5**. (b) Formation of 1D chain by water of crystallization in **5**.
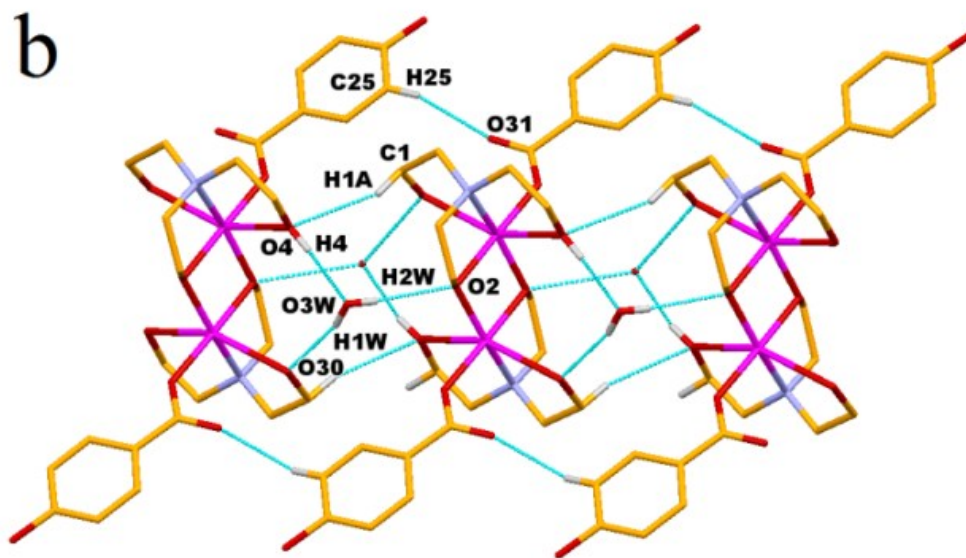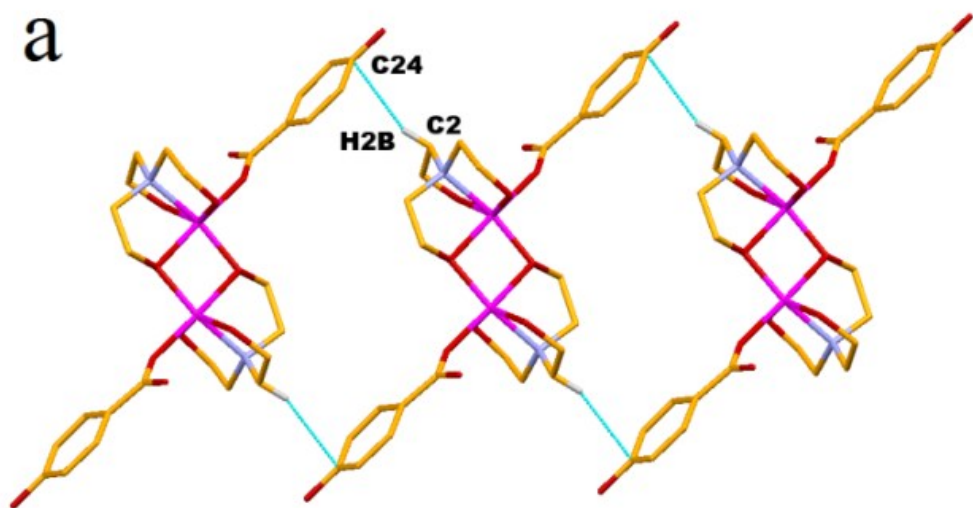
Fig. S5. (a) Formation of 1D chain by C–H⋯π interactions in **6**. (b) Formation of 1D chain by water of crystallization in **6**.

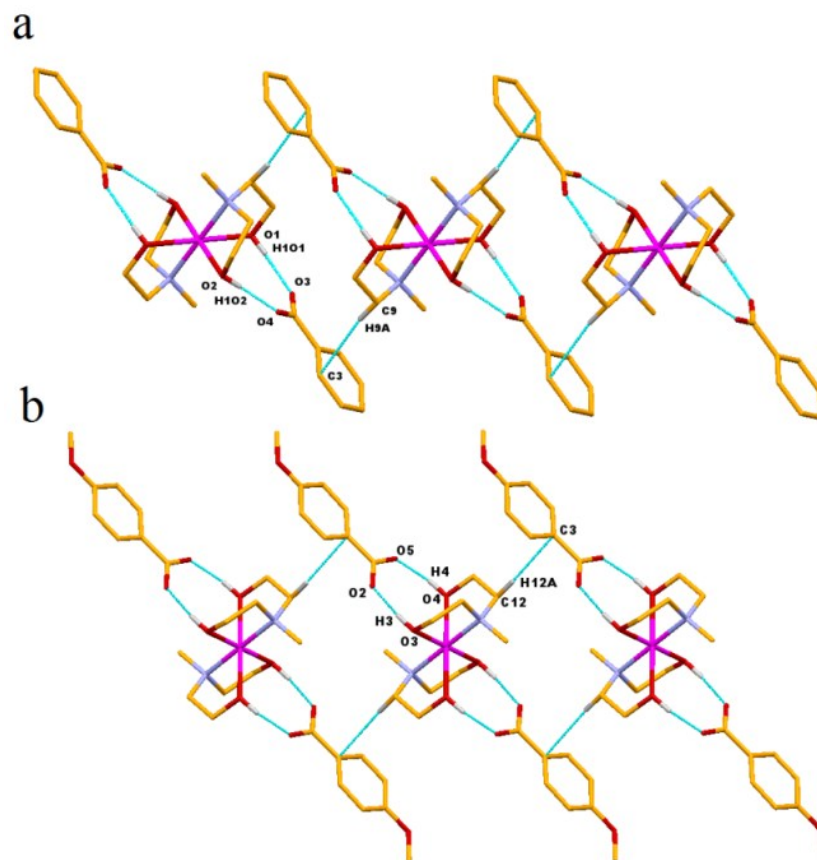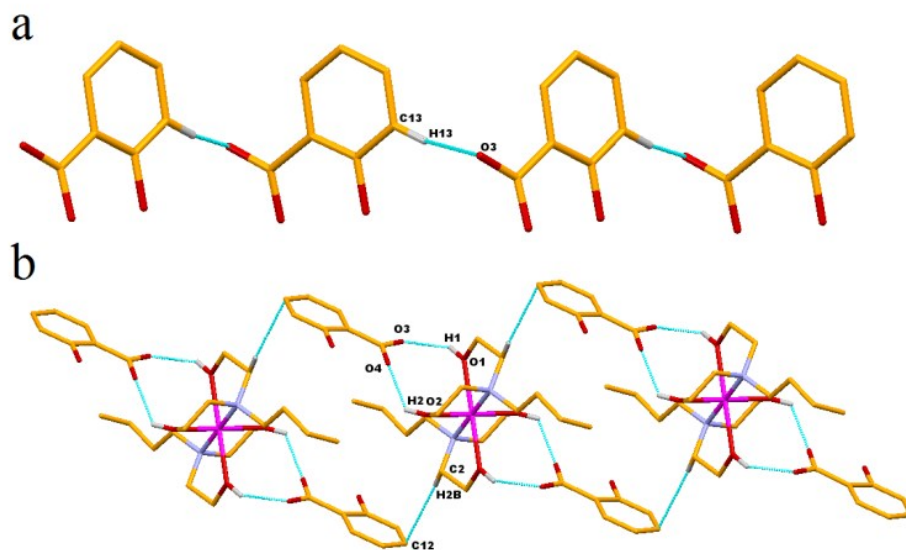Fig. S6. Formation of 1D chain by various O···H and C–H···π interactions in **7** (a) and **8** (b).

Fig. S7 (a) Formation of 1D chain by C–H···O interactions in **9** (b) Various O···H and C–H···π interactions in **9** resulting in a 2D sheet network.
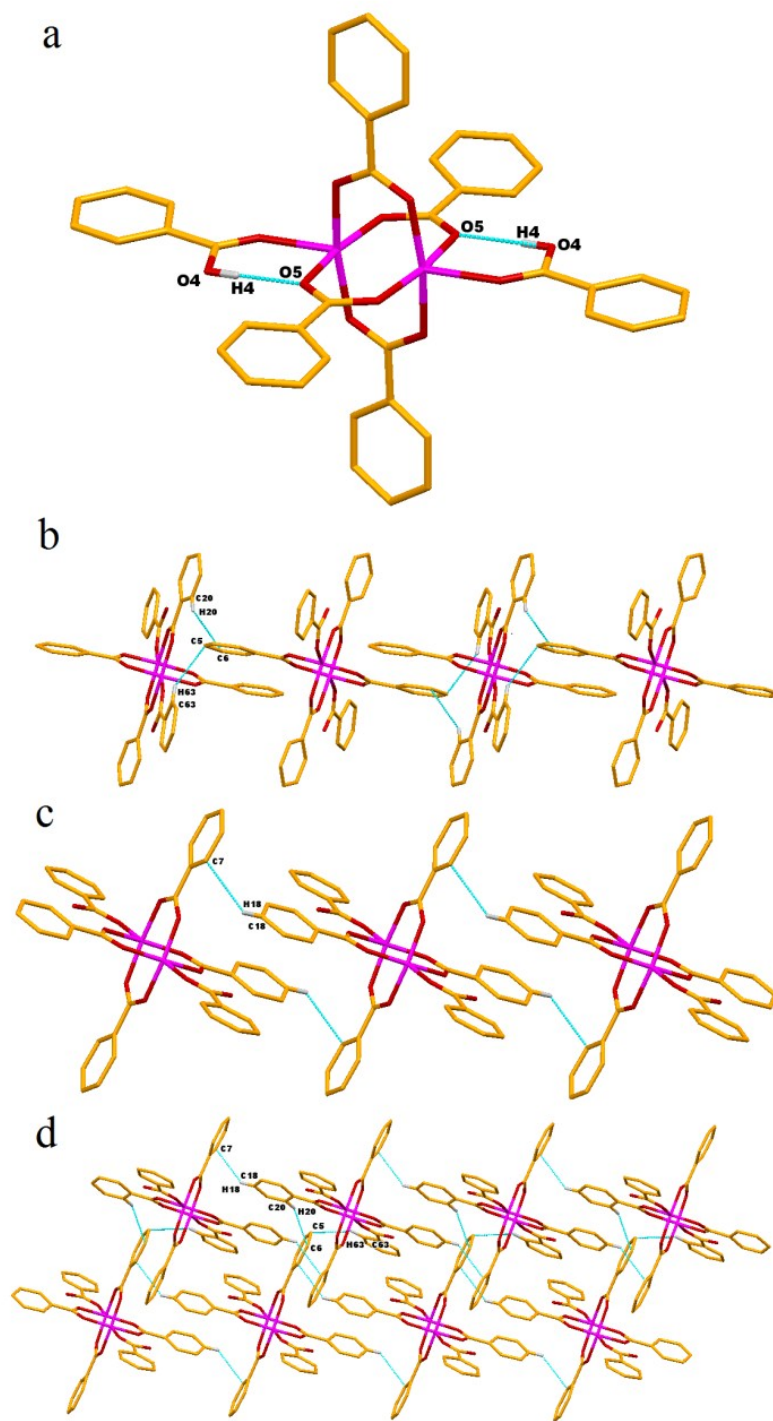
Fig. S8. (a) Intramolecular O–H⋯O interactions in **10**. (b) Formation of 1D chain by two different C–H⋯π interactions in **10**. (c) Formation of 1D chain by a C–H⋯π interaction in **10**. (d) Formation of 2D sheet network by all the three C–H⋯π interactions in **10**.

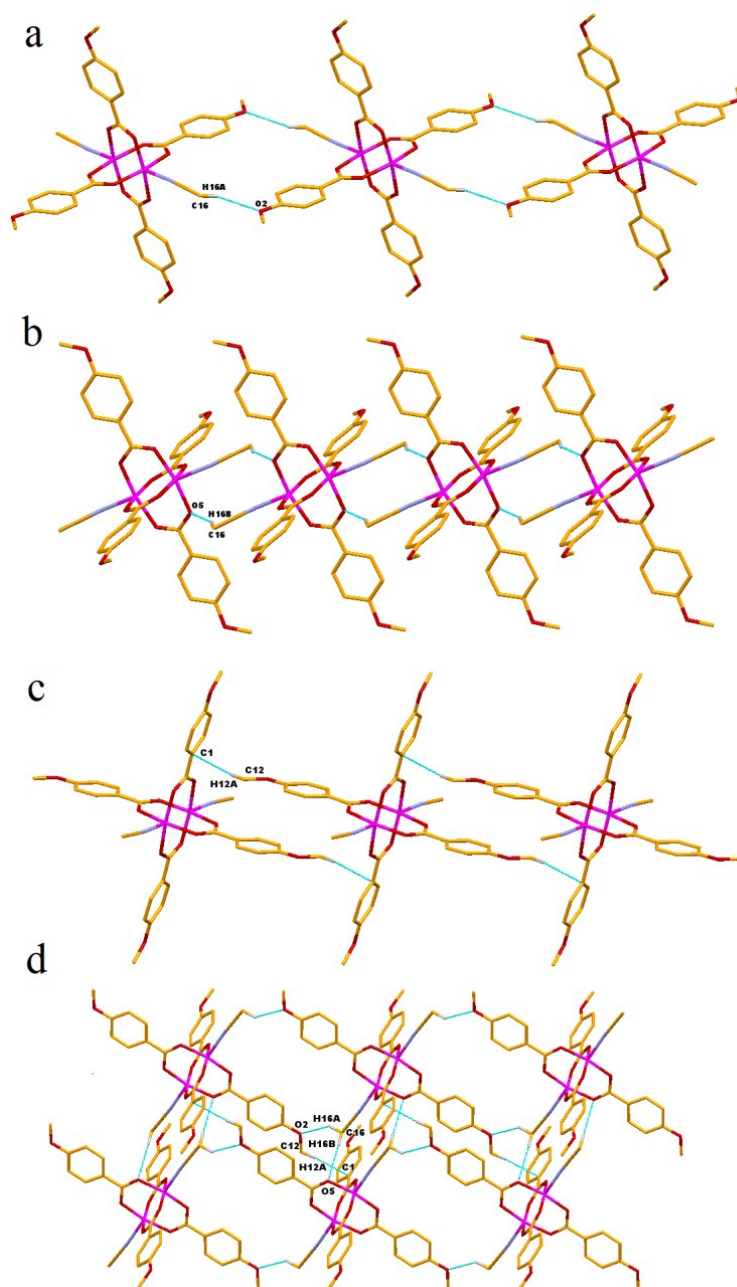Fig. S9. (a) Formation of 1D chain by C–H···O interactions in **11**. (b) Formation of 1D chain by C–H···O interaction in **11**. (c) Formation of 1D chain by C–H···π interactions in **11** (d) Formation of 2D sheet network by the combined C–H···O and C–H···π interactions in **11**.

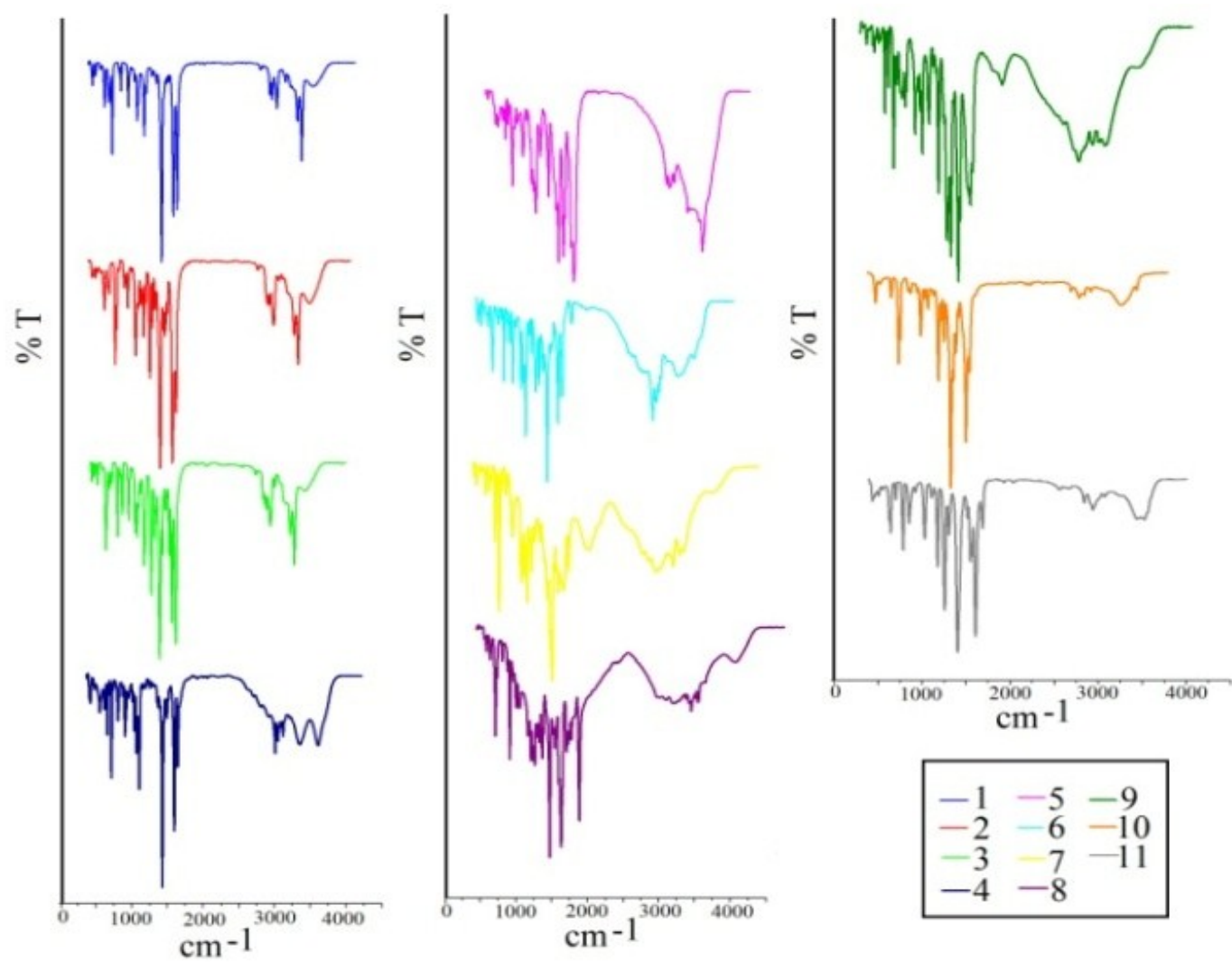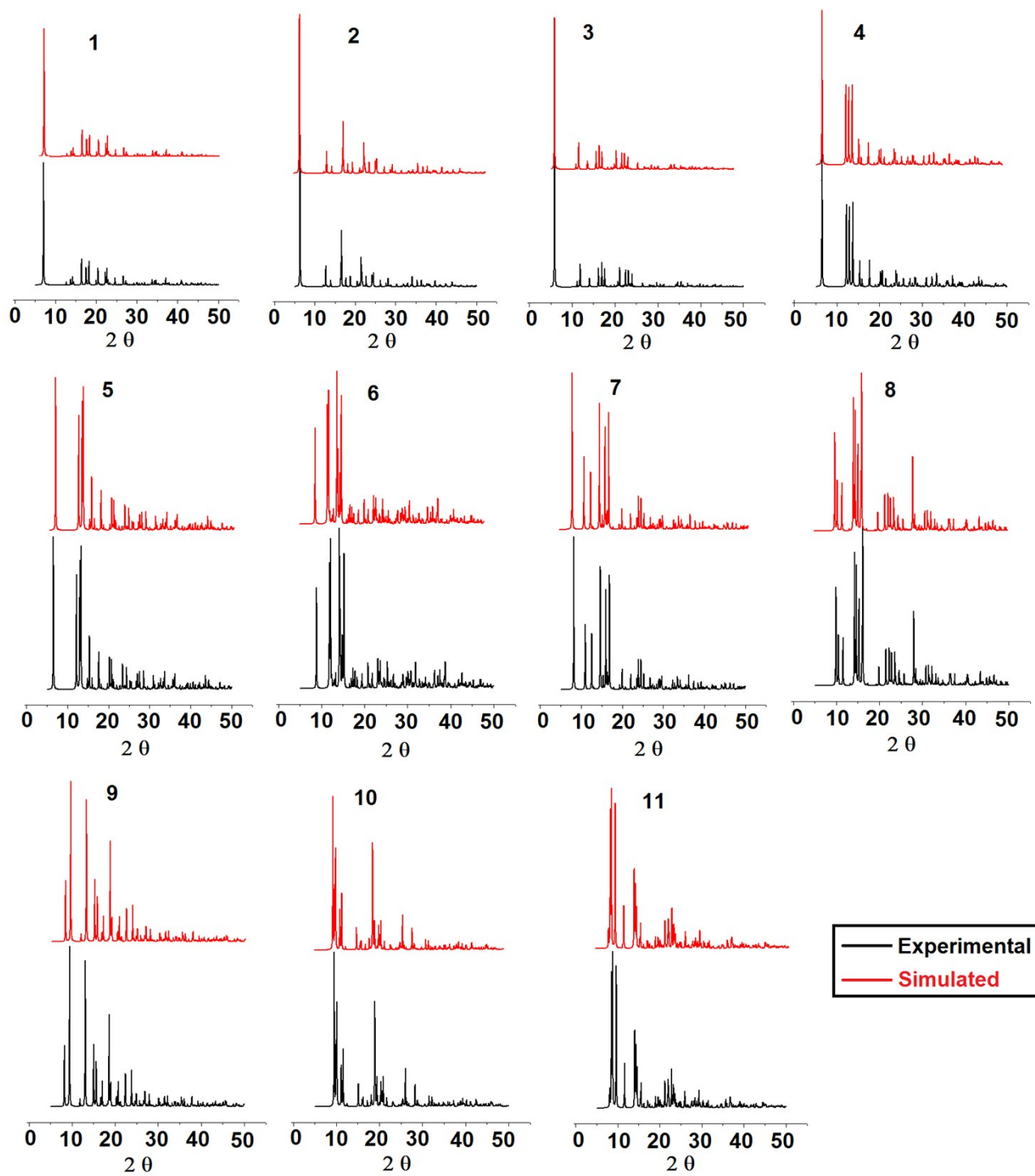Fig S10. FTIR spectra of **1–11**.

Fig. S11. As-synthesized and simulated PXRD patterns for **1–11**.
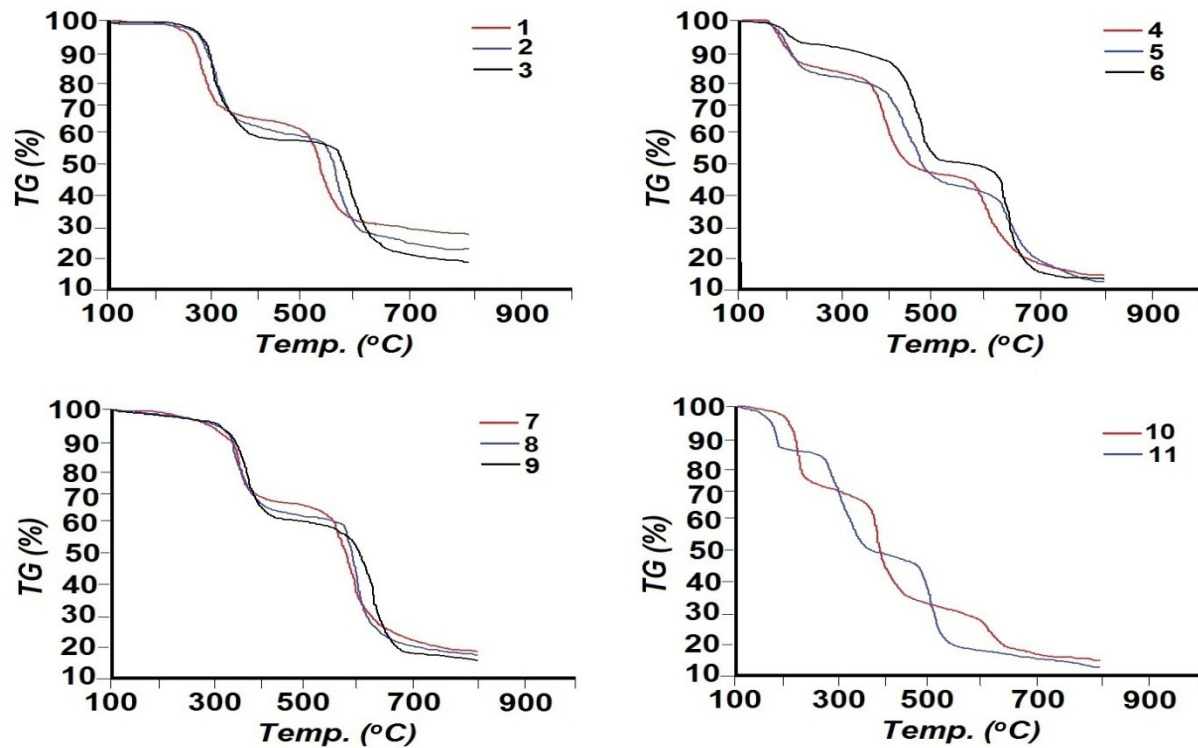
Fig. S12. Thermograms of **1**-**11**.
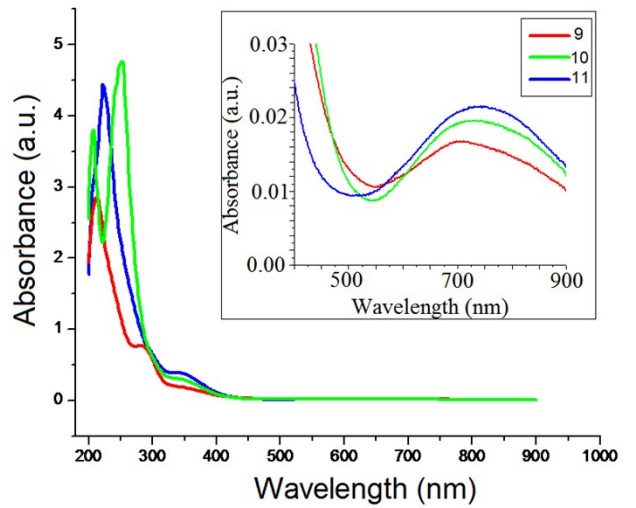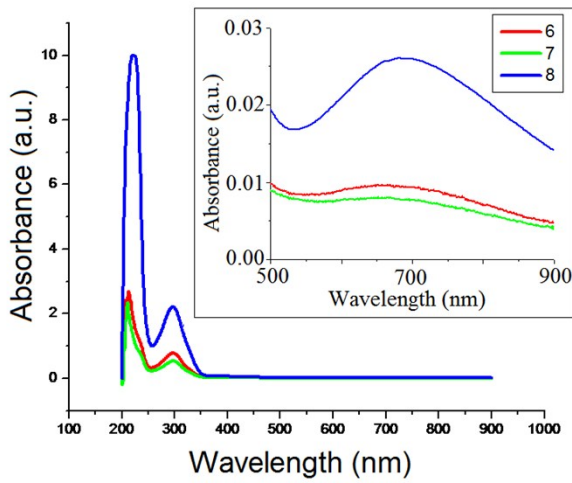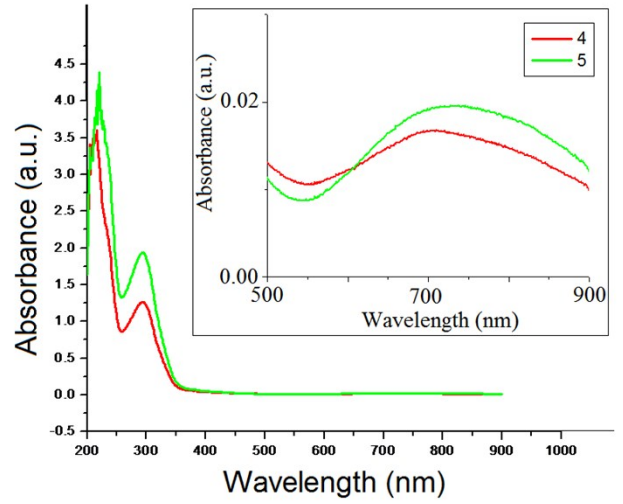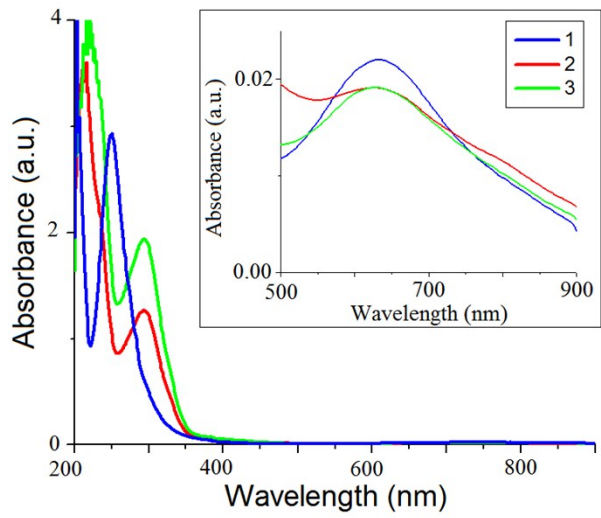
Fig S13. UV-visible spectra of **1**-**11**.
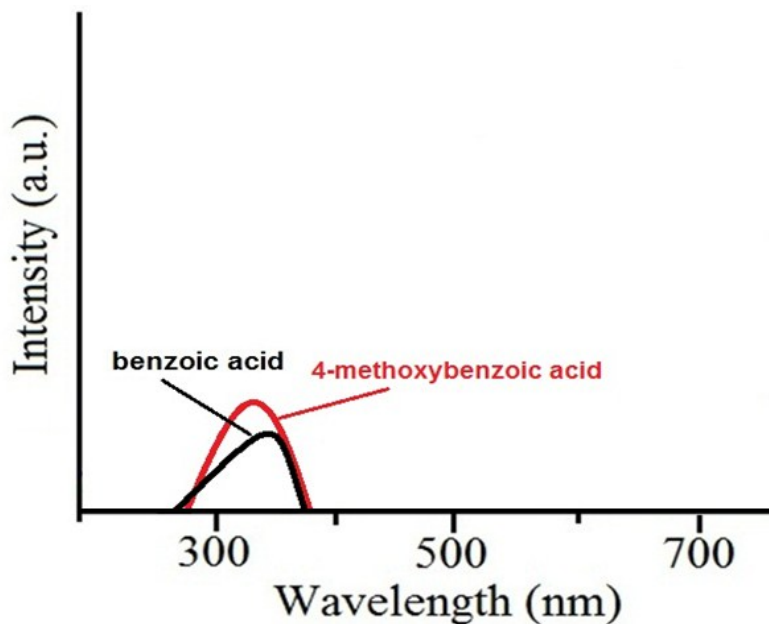
Fig. S14. Fluorescence spectra of benzoic acid and 4-methoxy benzoic acid recorded in 10^{-3} M methanol (λ_{ex} = 210 nm).

Quantum Yields:

Fluorescence quantum yields from fluorescence emission spectra of the complexes in methanol were calculated with quinine sulphate ($\varphi = 0.54$) as standard by using following equation:

$$\frac{\phi_{complex}}{\phi_{Q.S.}} = \frac{\text{Area of the complex}}{\text{Area of Q.S.}} \times \frac{\text{Absorbance of Q.S.}}{\text{Absorbance of complex}} \times \frac{\text{R. I. of solvent}}{\text{R. I. of water}}$$

Φ = quantum yield, R.I. = Refractive index, Q.S. = quinoline sulphate
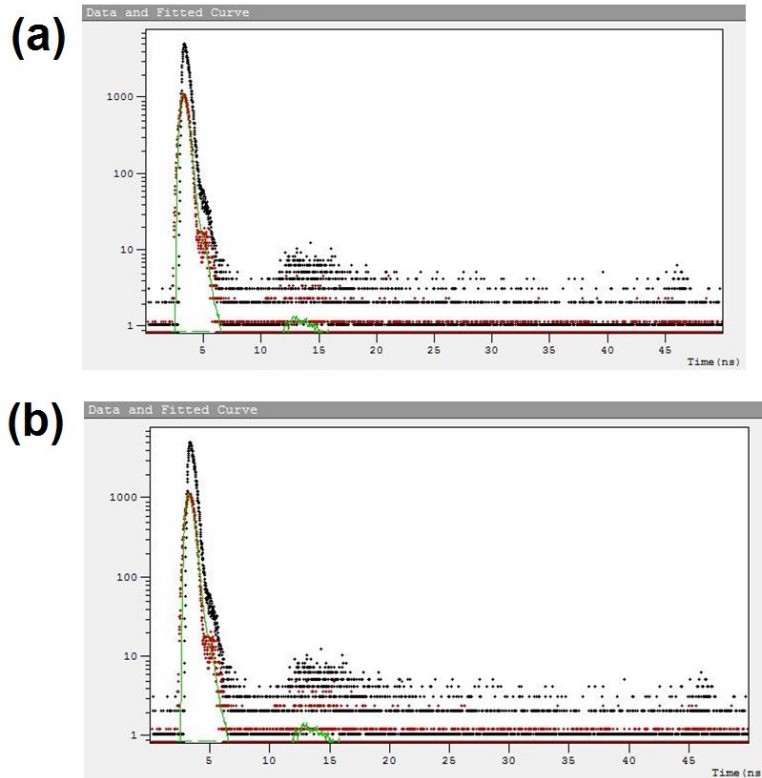
Fig. S15. Time resolved fluorescence (TRF) plot for (a) **7** and (b) **8**.
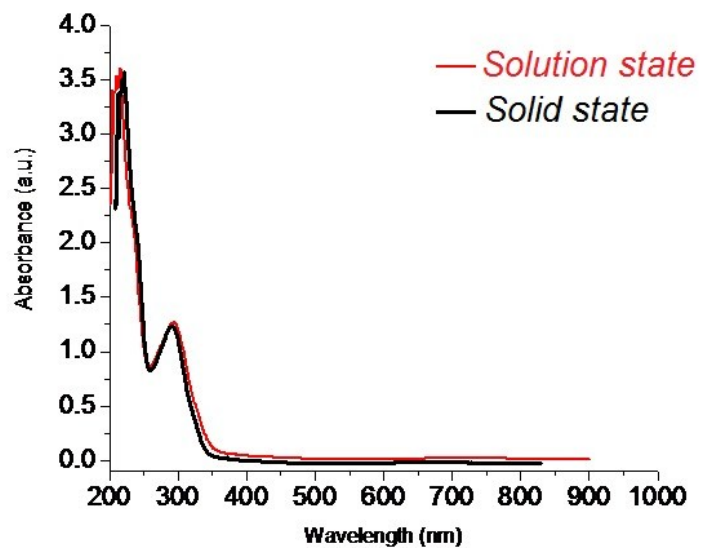
Fig. S16. Solid and solution (methanolic) state UV-Visible spectra of **4.**
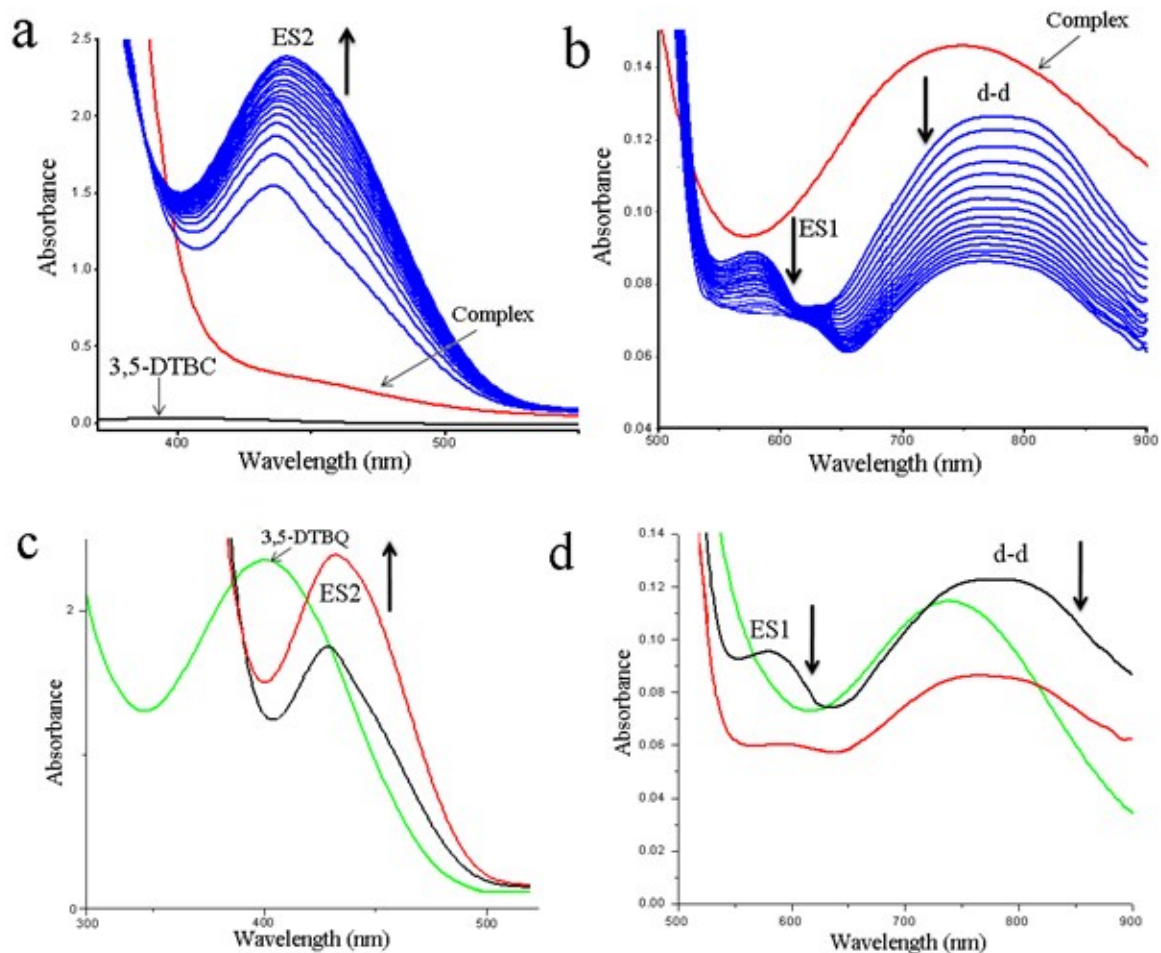
Fig. S17. (a) UV-vis spectra (300–500 nm) of **5** (10^{-4} M in MeOH); 3,5-DTBC (10^{-2} M in MeOH); changes in UV-vis spectra of **5** upon addition of 100 fold 3,5DTBC observed after each 5 min interval. (b) UV-vis spectra (500–900 nm) of **5** (10^{-4} M in MeOH); changes in UV-vis spectra of **5** upon addition of 100 fold 3,5-DTBC observed after each 5 min interval. (c) Changes in UV-vis spectra (300–500 nm) of **5** upon addition of 100 fold 3,5-DTBC observed: (1) immediately (black); (2) after 2 h (red) ; (3) after 3h (green). (d) Changes in UV-vis spectra (500–900 nm) of **5** upon addition of 100 fold 3,5-DTBC observed: (1) immediately (black); (2) after 2 h (red) ; (3) after 3h (green).
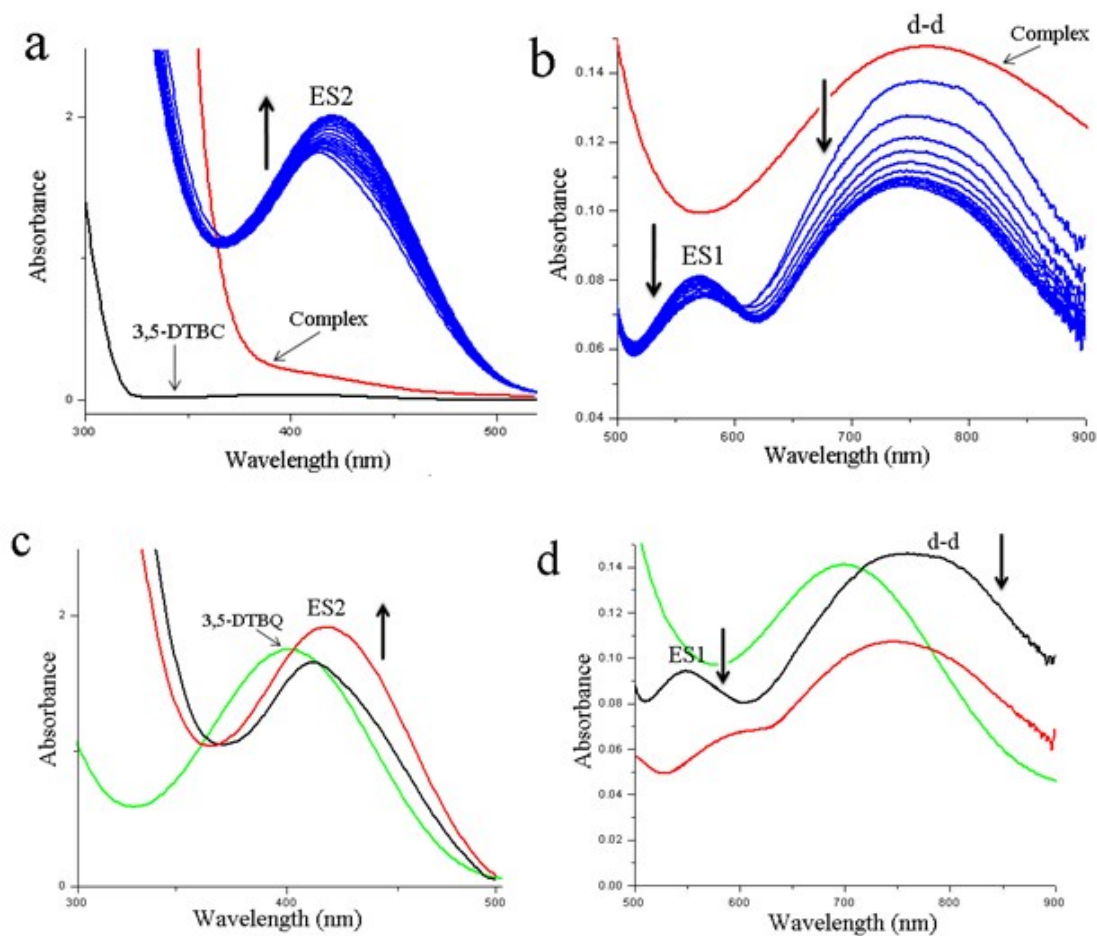
Fig. S18. (a) UV-vis spectra (300–500 nm) of **6** (10^{-4} M in MeOH); 3,5-DTBC (10^{-2} M in MeOH); changes in UV-vis spectra of **6** upon addition of 100 fold 3,5DTBC observed after each 5 min interval. (b) UV-vis spectra (500–900 nm) of **6** (10^{-4} M in MeOH); changes in UV-vis spectra of **6** upon addition of 100 fold 3,5-DTBC observed after each 5 min interval. (c) Changes in UV-vis spectra (300–500 nm) of **6** upon addition of 100 fold 3,5-DTBC observed: (1) immediately (black); (2) after 2 h (red) ; (3) after 3h (green). (d) Changes in UV-vis spectra (500–900 nm) of **6** upon addition of 100 fold 3,5-DTBC observed: (1) immediately (black); (2) after 2 h (red) ; (3) after 3h (green).
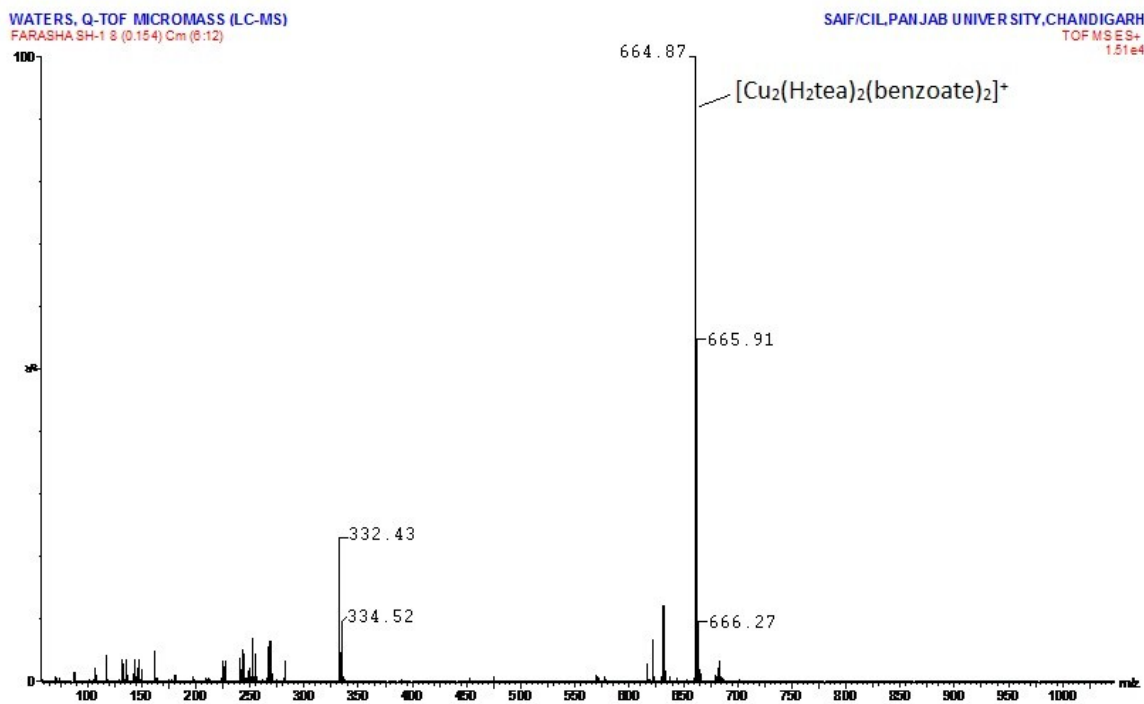
Fig. S19. Electrospray ionization mass spectrum (ESI-MS positive mode) of **4** in methanol.
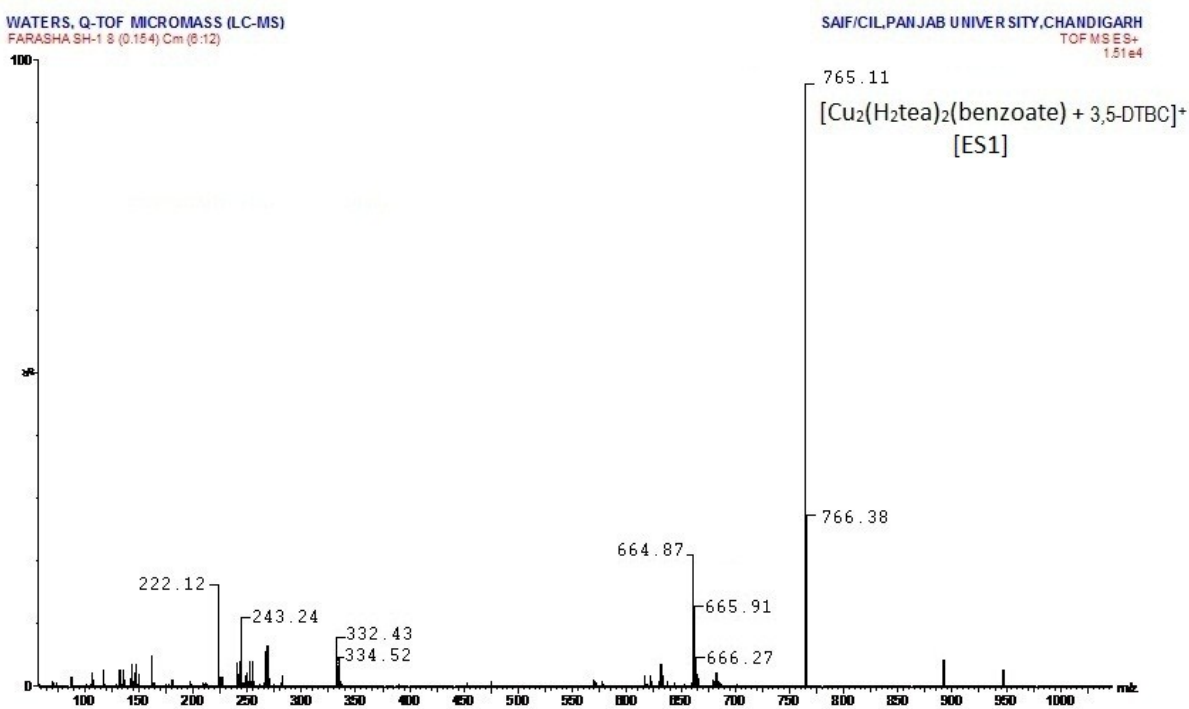

Fig. S20. Electrospray ionization mass spectrum (ESI-MS positive mode) of a 1:100 mixture of **4** and 3,5-DTBC in methanol, recorded immediately after addition of 3,5-DTBC to **4**.

644.32
$[Cu_2(H_2tea)_2 + 3,5\text{-}DTBC]^+$
[ES2]

765.11
$[Cu_2(H_2tea)_2(benzoate) + 3,5\text{-}DTBC]^+$
[ES1]

243.24

222.12

332.43
334.52

664.87
665.91
666.27

766.38

Fig. S21. Electrospray ionization mass spectrum (ESI-MS positive mode) of a 1:100 mixture of **4** and 3,5-DTBC in methanol, recorded after 2 hr.

243.24
$[Na\text{-}3,5DTBQ]^+$

644.32

765.11

Fig. S22. Electrospray ionization mass spectrum (ESI-MS positive mode) of a 1:100 mixture of **4** and 3,5-DTBC in methanol, recorded after 3 hr.

Fig S23. EPR spectra of **4** (a), **5** (b) and **6** (c) recorded at 20 minute intervals upto 2 hrs.

Table S1. Selected bond lengths and bond angles for **1**-**11**.

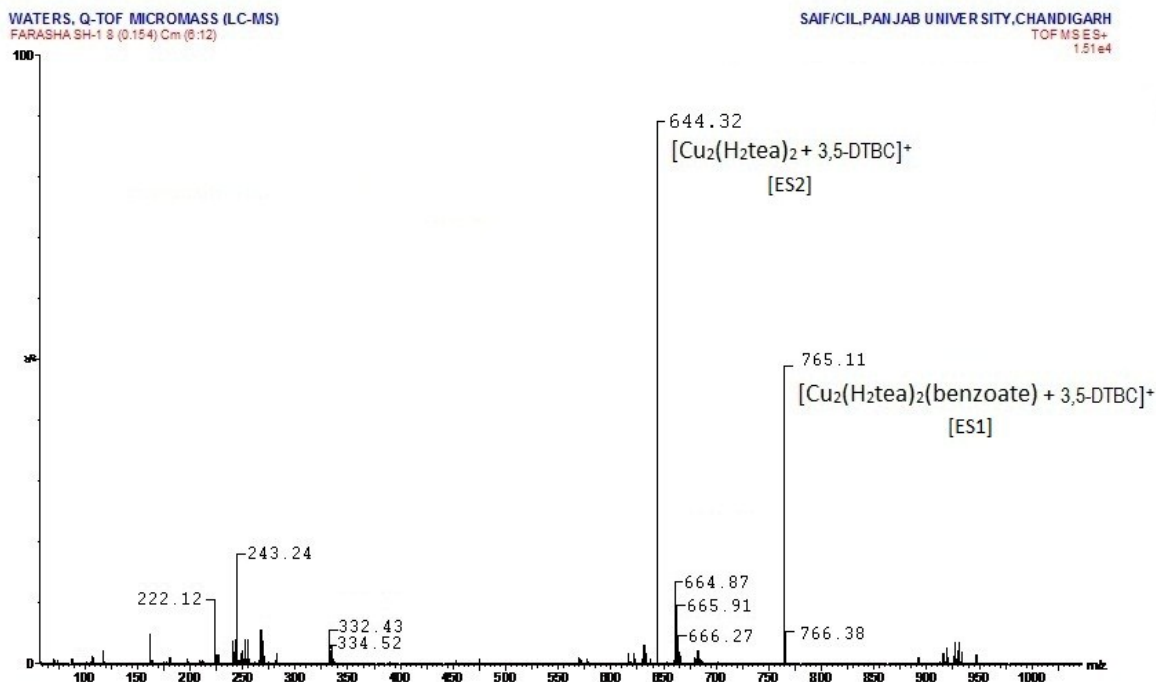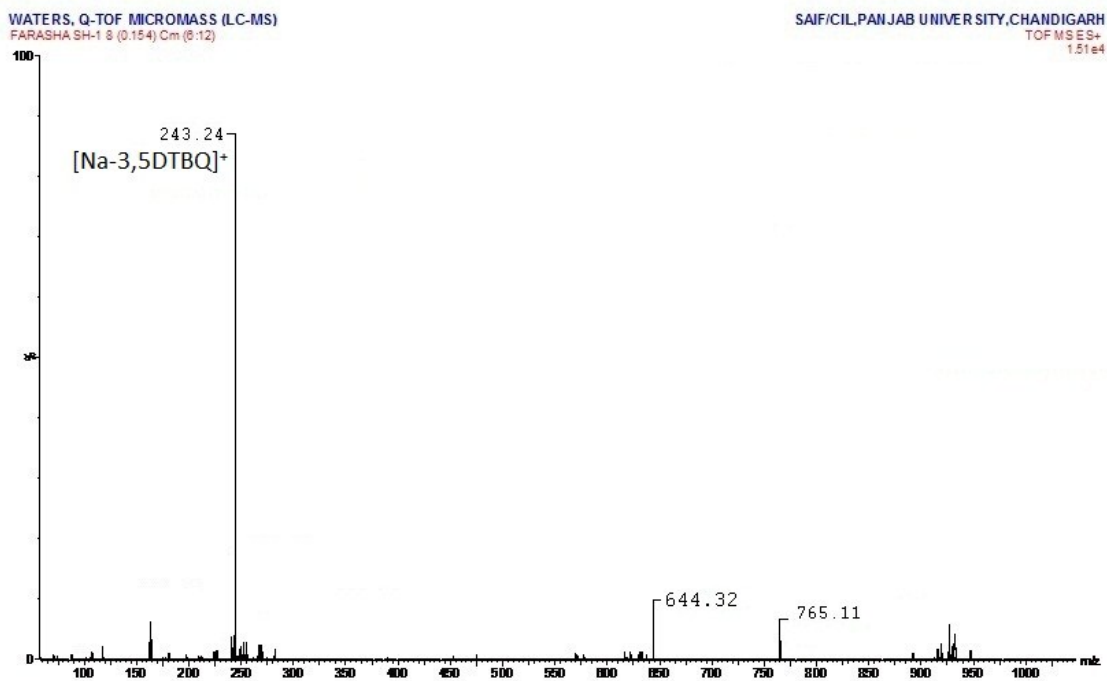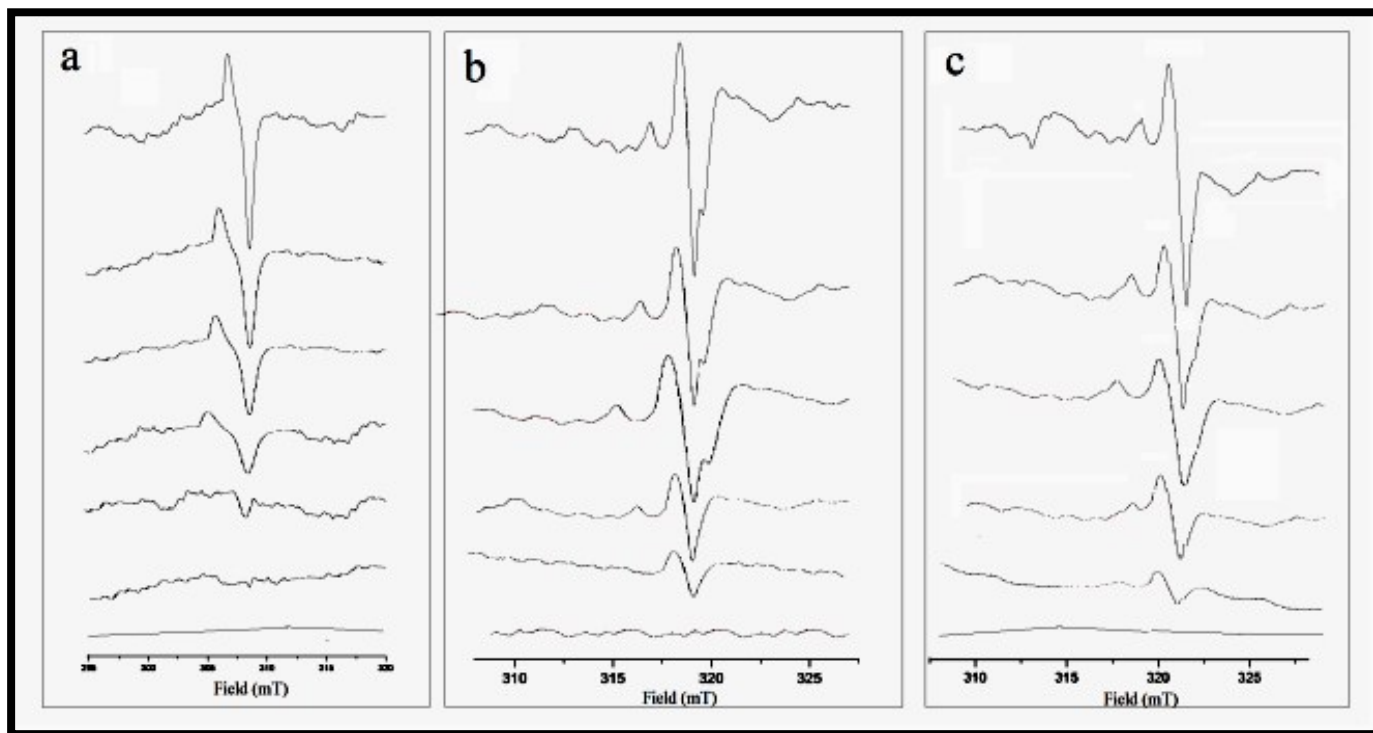| **1: bond lengths**	**2: bond lengths**	**3: bond lengths**
N1 Cu1 1.965(2)	Cu1 O1 1.9236(13)	Cu1 O1 1.9171(18)
O1 Cu1 1.9167(15)	Cu1 O1 1.9314(13)	Cu1 O2 1.9307(19)
O1 Cu1 1.9289(15)	Cu1 O2 1.9550(13)	Cu1 O1 1.9425(18)
O2 Cu1 1.9574(15)	Cu1 N1 1.9704(16)	Cu1 N1 1.965(2)
Cu1 Cu1 3.0316(5)	Cu1 Cu1 3.0445(4)	Cu1 Cu1 3.0351(7)
1: bond angles	**2: bond angles**	**3: bond angles**
Cu1 O1 Cu1 104.06(7)	O1 Cu1 O1 75.67(6)	O1 Cu1 O2 170.39(8)
O1 Cu1 O1 75.94(7)	O1 Cu1 O2 169.27(5)	O1 Cu1 O1 76.31(8)
O1 Cu1 O2 170.07(7)	O1 Cu1 O2 93.61(5)	O2 Cu1 O1 94.24(8)
O1 Cu1 O2 94.13(7)	O1 Cu1 N1 97.35(6)	O1 Cu1 N1 96.43(9)
O1 Cu1 N1 97.01(8)	O1 Cu1 N1 172.20(6)	O2 Cu1 N1 92.95(9)
O1 Cu1 N1 171.87(7)	O2 Cu1 N1 93.38(6)	O1 Cu1 N1 172.46(9)
O2 Cu1 N1 92.89(8)	O1 Cu1 Cu1 37.93(4)	O1 Cu1 Cu1 38.45(5)
O1 Cu1 Cu1 38.11(4)	O1 Cu1 Cu1 37.75(4)	O2 Cu1 Cu1 132.07(6)
O1 Cu1 Cu1 37.83(4)	O2 Cu1 Cu1 131.35(4)	O1 Cu1 Cu1 37.86(5)
O2 Cu1 Cu1 131.96(5)	N1 Cu1 Cu1 135.18(5)	N1 Cu1 Cu1 134.85(7)
N1 Cu1 Cu1 134.99(6)	C4 O2 Cu1 109.76(11)	Cu1 O1 Cu1 103.70(8)

4: bond lengths	**5: bond angles**	**6: bong angles**
N1 Cu1 2.048(2)	O5 Cu1 O5 83.10(7)	O6 Cu1 O6 83.09(5)
O1 Cu1 1.9579(17)	O5 Cu1 O3 94.99(7)	O6 Cu1 O1 94.45(5)
O1W H1WA 0.8700	O5 Cu1 O3 177.57(6)	O6 Cu1 O1 177.03(5)
O1W H1WB 0.8701	O5 Cu1 N1 161.72(8)	O6 Cu1 N1 161.31(5)
O3 Cu1 1.9386(17)	O5 Cu1 N1 84.96(7)	O6 Cu1 N1 84.53(5)
O3 Cu1 1.9451(17)	O3 Cu1 N1 97.25(7)	O1 Cu1 N1 98.25(5)
O4 H4A 0.75(3)		O6 Cu1 Cu1 41.58(3)
O5 H5A 0.8400		O6 Cu1 Cu1 41.52(3)
Cu1 Cu1 2.9157(6)		O1 Cu1 Cu1 136.01(4)
4: Bond angles		N1 Cu1 Cu1 124.66(3)
O3 Cu1 O3 82.69(8)	**6: bond lengths**	O9 Cu2 O9 180.0
O3 Cu1 O1 95.12(8)	Cu1 O6 1.9419(10)	O9 Cu2 N2 94.42(5)
O3 Cu1 O1 177.22(8)	Cu1 O6 1.9440(10)	O9 Cu2 N2 85.58(5)
O3 Cu1 N1 161.49(8)	Cu1 O1 1.9501(11)	O9 Cu2 N2 85.58(5)
O3 Cu1 N1 84.64(8)	Cu1 N1 2.0548(12)	O9 Cu2 N2 94.42(5)
O1 Cu1 N1 97.88(8)	Cu1 Cu1 2.9083(3)	N2 Cu2 N2 180.0
O3 Cu1 Cu1 41.43(5)	Cu2 O9 1.9486(10)	
O3 Cu1 Cu1 41.26(5)	Cu2 O9 1.9486(10)	
O1 Cu1 Cu1 136.52(6)	Cu2 N2 2.0836(13)	
N1 Cu1 Cu1 124.63(6)	Cu2 N2 2.0837(13)	
5: bond lengths		
Cu1 O5 1.9365(15)		
Cu1 O5 1.9464(15)		
Cu1 O3 1.9683(15)		
Cu1 N1 2.0422(18)		

7: bond lengths	10: bond lengths	11: bong angles
N1 Cu1 2.0374(14)	O1 Cu1 2.1952(14)	C9 O5 Cu1 122.97(15)
O1 Cu1 2.3499(17)	O3 Cu1 1.9980(13)	C13 O6 C16 118.2(3)
O1 H1 0.875(9)	O4 Cu1 1.9507(13)	C1 O2 Cu1 121.70(15)
O2 Cu1 1.9946(13)	O5 Cu1 1.9535(13)	C5 O3 C8 119.0(2)
O2 H2 0.865(9)	O6 Cu1 1.9454(13)	C9 O4 Cu1 123.30(15)
7: bond angles	Cu1 Cu1 2.6066(5)	C1 O1 Cu1 124.28(15)
C12 N1 Cu1 111.77(12)	**10: bond angles**	O5 Cu1 O1 88.74(7)
C9 N1 Cu1 106.98(11)	C1 O1 Cu1 130.14(13)	O5 Cu1 O4 168.59(7)
C10 N1 Cu1 106.90(11)	C8 O3 Cu1 123.84(12)	O1 Cu1 O4 89.92(8)
C8 O1 Cu1 107.45(11)	C8 O4 Cu1 123.65(12)	O5 Cu1 O2 89.78(7)
8: bond lengths	C15 O5 Cu1 123.61(12)	O1 Cu1 O2 168.63(7)
N1 Cu1 2.0423(15)	C15 O6 Cu1 122.05(12)	O4 Cu1 O2 89.30(8)
O1 Cu1 1.9986(14)	O6 Cu1 O4 89.09(6)	O5 Cu1 N1 96.67(8)
O1 H1 0.72(2)	O6 Cu1 O5 169.13(6)	O1 Cu1 N1 95.04(8)
O2 Cu1 2.3628(16)	O4 Cu1 O5 90.42(6)	O4 Cu1 N1 94.74(8)
8: bond angles	O6 Cu1 O3 88.91(6)	O2 Cu1 N1 96.33(8)
C10 N1 Cu1 107.30(13)	O4 Cu1 O3 168.81(5)	O5 Cu1 Cu1 84.61(5)
C13 N1 Cu1 111.45(13)	O5 Cu1 O3 89.48(6)	O1 Cu1 Cu1 83.51(5)
C11 N1 Cu1 107.20(13)	O6 Cu1 O1 94.70(6)	O4 Cu1 Cu1 83.98(5)
C9 O1 Cu1 107.84(12)	O4 Cu1 O1 100.68(6)	O2 Cu1 Cu1 85.13(5)
C12 O2 Cu1 107.77(13)	O5 Cu1 O1 96.06(6)	N1 Cu1 Cu1 178.05(6)
Cu1 O2 H2 112(2)	O3 Cu1 O1 90.46(5)	
O1 Cu1 O1 180.0	O6 Cu1 Cu1 85.38(4)	
O1 Cu1 N1 85.08(6)	O4 Cu1 Cu1 85.67(4)	
O1 Cu1 N1 94.92(6)	O5 Cu1 Cu1 83.75(4)	
O1 Cu1 N1 94.92(6)	O3 Cu1 Cu1 83.19(4)	
O1 Cu1 N1 85.08(6)	O1 Cu1 Cu1 173.65(4)	
N1 Cu1 N1 180.0	Cu1 O1 H1 122.4(11)	
O1 Cu1 O2 94.70(6)	C11 O2 Cu1 106.64(11)	
O1 Cu1 O2 85.30(6)	Cu1 O2 H2 124.9(11)	
N1 Cu1 O2 78.25(6)	O2 Cu1 O2 180.0	
N1 Cu1 O2 101.75(6)	O2 Cu1 N1 94.71(6)	
O1 Cu1 O2 85.30(6)	O2 Cu1 N1 85.29(6)	
O1 Cu1 O2 94.70(6)	O2 Cu1 N1 85.29(6)	
N1 Cu1 O2 101.75(6)	O2 Cu1 N1 94.71(6)	
N1 Cu1 O2 78.25(6)	N1 Cu1 N1 180.00(6)	
O2 Cu1 O2 180.0	O2 Cu1 O1 87.06(6)	
9: bond lengths	O2 Cu1 O1 92.94(6)	
Cu1 O1 2.0301(17)	N1 Cu1 O1 79.37(6)	
Cu1 O1 2.0301(18)	N1 Cu1 O1 100.63(6)	
Cu1 N1 2.030(2)	O2 Cu1 O1 92.94(6)	
Cu1 N1 2.030(2)	O2 Cu1 O1 87.06(6)	
Cu1 O2 2.3233(18)	N1 Cu1 O1 100.63(6)	
Cu1 O2 2.3234(18)	N1 Cu1 O1 79.37(6)	
9: bond angles	O1 Cu1 O1 180.0	
O1 Cu1 O1 180.00(9)	**11: bond lengths**	
O1 Cu1 N1 85.42(8)	N1 Cu1 2.206(2)	
O1 Cu1 N1 94.58(8)	C21 N3 1.023(9)	
O1 Cu1 N1 94.58(8)	C21 C22 1.356(10)	
O1 Cu1 N1 85.42(8)	O5 Cu1 1.9549(15)	
N1 Cu1 N1 180.00(13)	O2 Cu1 1.9660(16)	
O1 Cu1 O2 93.80(7)	O4 Cu1 1.9634(16)	
O1 Cu1 O2 86.20(7)	O1 Cu1 1.9573(16)	
N1 Cu1 O2 80.88(7)	Cu1 Cu1 2.6253(5)	
N1 Cu1 O2 99.13(7)	C22 H22A 0.9800	
O1 Cu1 O2 86.20(7)	C22 H22B 0.9800	
O1 Cu1 O2 93.79(7)	C22 H22C 0.9800	
N1 Cu1 O2 99.13(7)		
N1 Cu1 O2 80.87(7)		
O2 Cu1 O2 180.0		